LHCb-PHYS-2007-030
13 April 2007

Study of radiative penguin decays $\mathrm{B}^0 \to \mathrm{K}^{*0}\gamma$ and $\mathrm{B}^0_\mathrm{s} \to \phi\gamma$ at LHCb

Lesya Shchutska[1,†], Andrey Golutvin[2,1] and Ivan Belyaev[3,1]

[1]*ITEP, Moscow, Russia*
[2]*CERN, Switzerland*
[3]*Syracuse University, USA*

Abstract

The updated selection for decays $\mathrm{B}^0 \to \mathrm{K}^{*0}\gamma$ and $\mathrm{B}^0_\mathrm{s} \to \phi\gamma$ is presented.

[†]E-mail: Lesya.Shchutska@cern.ch

1 Introduction

Radiative penguin B decays provide a sensitive test of the Standard Model (SM). These transitions are induced by flavour changing neutral currents and are sensitive to new couplings from beyond the SM physics.

One way of searching for new phenomena is a systematic study of CP violation in radiative B decays. This may occur via one of two mechanisms. Direct CP violation (CPV) results in a difference of the decay rates $\mathrm{B} \to \mathrm{X}\gamma$ and $\bar{\mathrm{B}} \to \bar{\mathrm{X}}\gamma$. In the SM due to the very small u-quark contribution to a penguin loop, the direct CP asymmetry is reliably predicted to be $\leq 1\%$ for $\mathrm{b} \to \mathrm{s}\gamma$ and $< 16\%$ for $\mathrm{b} \to \mathrm{d}\gamma$ transitions [1]. In some SM extensions, the contribution from new particles in the loop may result in up to $10\% - 40\%$ direct CP asymmetry [2]. The theoretical prediction for the inclusive decays is rather clean. However the experimentally accessible exclusive cases are theoretically much more difficult to calculate. Another test of the SM can be made by measuring the mixing induced CP violation which occurs when both $\mathrm{B}^0_{(\mathrm{s})}$ and $\bar{\mathrm{B}}^0_{(\mathrm{s})}$ have transitions to the same final state $\mathrm{X}^0\gamma$ (X^0 is undistinguishable from $\bar{\mathrm{X}}^0$) and interference takes place between mixing and decay amplitudes [3]. A recent review on the status of these CPV measurements can be found in [4]. At present, mixing induced CP violation has been searched in $\mathrm{B}^0 \to K^{*0}\gamma$ followed by $\mathrm{K}^{*0} \to \mathrm{K}^0_{\mathrm{S}}\pi^0$ in B-factories [5, 6]. No significant CP violation is seen. This is consistent with the SM expectations quoted above. With the LHCb detector, mixing induced CP violation can be searched for in $\mathrm{B}^0 \to \rho^0\gamma$ (or through the equivalent non-resonant mode [7]) and $\mathrm{B}^0_{\mathrm{s}} \to \phi\gamma$.

Radiative B decays give information on the ratio of CKM matrix elements $|\mathrm{V_{td}}/\mathrm{V_{ts}}|$ with reduced hadronic uncertainties [8]. This ratio can be extracted from the ratio of branching fractions of $\mathrm{B}^0 \to \rho^0\gamma$ to $\mathrm{B}^0 \to \mathrm{K}^{*0}\gamma$ decays. Presently the most precise measurements are made by Belle [9] and BaBar [10] collaborations.

The decay $\mathrm{B}^0 \to \mathrm{K}^{*0}\gamma$ has been measured by Belle [11], BaBar [12] and CLEO [13] collaborations. The results are in good agreement with theoretical predictions [14].

The LHCb experiment can complement the existing observations by studying radiative $\mathrm{B}^0_{\mathrm{s}}$ decays while substantially improving the present results by measuring CP violation in decays involving $\mathrm{b} \to \mathrm{d}\gamma$ transitions. The results presented in this paper are the continuation of the previous study [15] with improved Monte Carlo simulation.

2 Reconstruction and selection

The present study uses samples of generated $\mathrm{B}^0 \to \mathrm{K}^{*0}\gamma$ and $\mathrm{B}_\mathrm{s}^0 \to \phi\gamma$ events, followed by $\mathrm{K}^{*0} \to \mathrm{K}^+\pi^-$ and $\phi \to \mathrm{K}^+\mathrm{K}^-$, where the $\mathrm{B}_{\mathrm{d,s}}$-mesons are produced within the 400 mrad cone of the LHCb acceptance[1] [16]. The selection procedure is mainly based on using the two-body kinematics of the relevant decays and various geometrical cuts on the primary vertices of the pp-interaction (PV) and B-decay secondary vertices (SV). The main source of background is assumed to be $\mathrm{b\bar{b}}$-inclusive events where at least one b-hadron is emitted in the LHCb acceptance region. The LHCb $\mathrm{b\bar{b}}$ data sample consists of 34 million simulated events processed as if they were real data. This corresponds to 13 minutes of running at the nominal luminosity of $2 \times 10^{32}\mathrm{cm}^{-2}\mathrm{s}^{-1}$.

The selection criteria have been chosen to maximize the ratio,

$$\xi = \frac{\mathcal{S}}{\sqrt{\mathcal{S}+\mathcal{B}}}. \tag{1}$$

Here $\mathcal{S}$ and $\mathcal{B}$ stand for the number of signal and background events, respectively (see Appendix for details).

Since the reconstruction algorithms for $\mathrm{B}^0 \to \mathrm{K}^{*0}\gamma$ and $\mathrm{B}_\mathrm{s}^0 \to \phi\gamma$ are very much alike they are described in parallel.

Photons are identified as neutral clusters in the electromagnetic calorimeter ECAL [17], that are not associated with charged tracks [18]. The two-body kinematics of the signal decays results in a hard transverse energy spectra of photons. In order to discriminate between the signal and the background from soft photons, which are produced in the numerous π^0 decays in the pp-collision, the transverse energy of the photon, $\mathrm{E}_\mathrm{T}^\gamma$, is required to be greater than $2.8\ \mathrm{GeV}$. The dependence of the ratio ξ on the cut value is presented in Figure 1. The optimal value is close to the actual threshold of the dedicated low level trigger for photons with high transverse energy [19].

Pions and kaons are identified using the difference in logarithmic likelihoods between assigning the pion, kaon and proton hypothesis to the tracks reconstructed in the RICH detector [20]. The identification procedure is described in detail elsewhere [16]. Charged tracks are considered as pion candidates if $\Delta\log\mathcal{L}_{\pi\mathrm{K}} = \log\frac{\mathcal{P}(\pi)}{\mathcal{P}(\mathrm{K})} > -5$. As shown in Figure 2a, the ξ function shows no maximum. Therefore, the standard LHCb cut is applied. For kaons, the cut on $\Delta\log\mathcal{L}$ depends on whether the kaon is used to reconstruct the K^{*0} or ϕ meson. Kaons produced in K^{*0} decays and in ϕ decays are selected with the criteria $\Delta\log\mathcal{L}_{\mathrm{K}\pi} > 0$,

[1] Charged conjugates are implied throughout the paper.

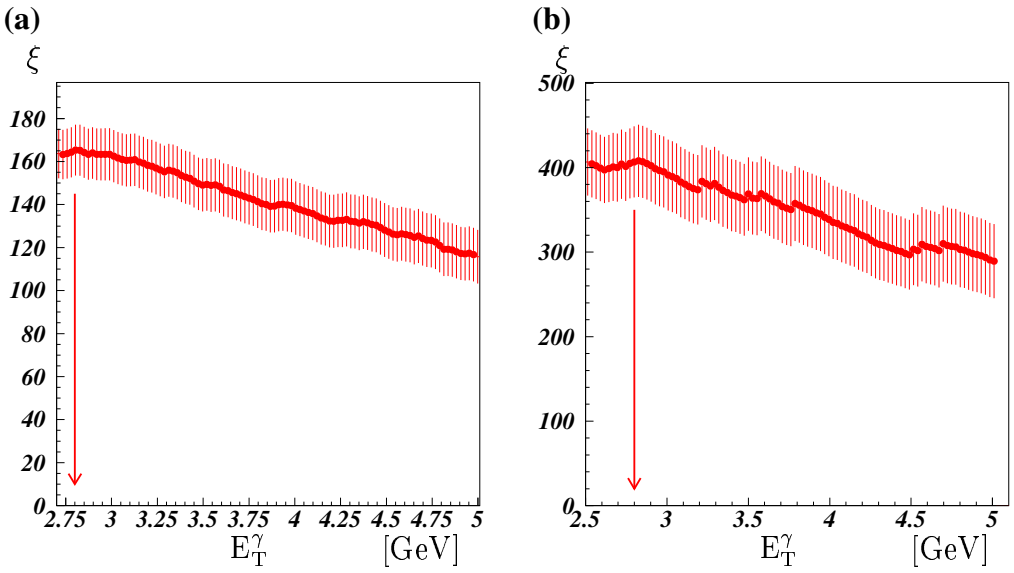

Figure 1: The ratio ξ as a function of the cut value on $\mathrm{E}_\mathrm{T}^\gamma$, the rest of the cuts is applied. The arrow points to the chosen value of the $\mathrm{E}_\mathrm{T}^\gamma$ cut. a) $\mathrm{B}^0 \to \mathrm{K}^{*0}\gamma$, b) $\mathrm{B}_\mathrm{s}^0 \to \phi\gamma$.

$\Delta \log \mathcal{L}_{\mathrm{Kp}} > 5$ (see Figure 3) and $\Delta \log \mathcal{L}_{\mathrm{K}\pi} > 3$ (see Figure 2b) respectively. In the latter case no cut on $\Delta \log \mathcal{L}_{\mathrm{Kp}}$ is applied.

Due to the relatively long lifetime of B mesons, the B production and decay vertices are spatially separated such that the products of B decays do not point to the production vertex. This fact is used to reject tracks originating from a primary vertex. It is demanded that the significance of the impact parameter $\chi^2_{\mathrm{IP}} = (\mathrm{IP}/\sigma_{\mathrm{IP}})^2$ of each of the two charged tracks with respect to all reconstructed primary vertices has to be larger than 25 ($\chi^2_{\mathrm{IP}} > 25$). The dependence of the ratio ξ on the cut value of χ^2_{IP} is shown in Figure 4.

An unconstrained vertex fit is performed to form K^{*0} and ϕ candidates. The distributions of the significance of the χ^2_{VX} vertex fit for signal decays and the dependence of the ratio ξ on the cut value of χ^2_{VX} are presented in Figures 5 and 6 for $\mathrm{B}^0 \to \mathrm{K}^{*0}\gamma$ and $\mathrm{B}_\mathrm{s}^0 \to \phi\gamma$ decays respectively. Both distributions show very wide maxima[2]. For both signal decays χ^2_{VX} is required to be smaller than nine ($\chi^2_{\mathrm{VX}} < 9$) which coinsides with the value used at the event preselection level.

The mass windows for K^{*0} and ϕ candidates were chosen to be ± 55 MeV$/c^2$

[2]The detailed study of the background events in section 3.1 shows that the major background is due to $\mathrm{K}\pi(\mathrm{KK})$ combinations from the same vertices, which explains these wide maxima.

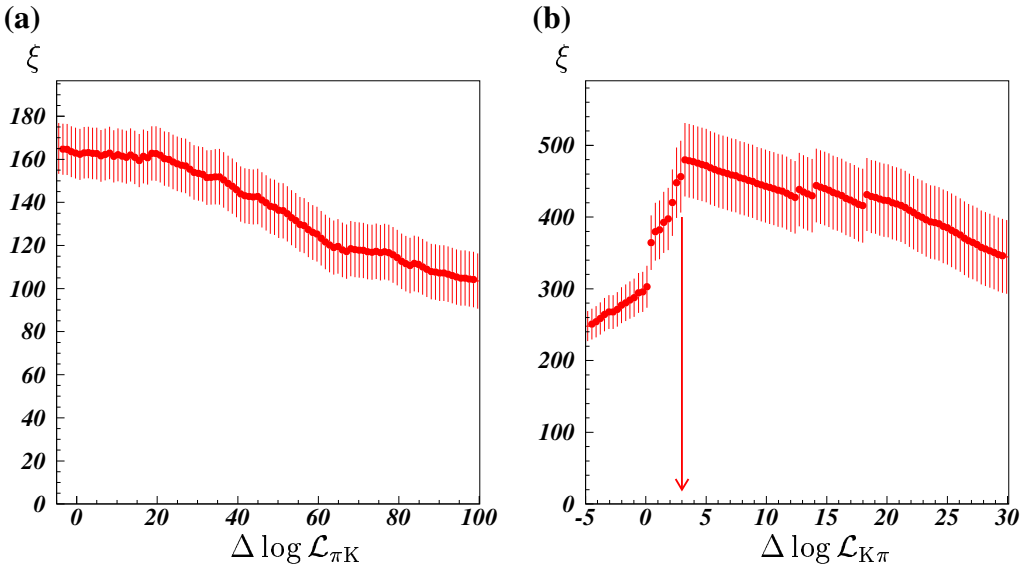

Figure 2: a) Pion identification for $B^0 \to K^{*0}\gamma$. Optimization ratio ξ as a function of cut value of $\Delta \log \mathcal{L}_{\pi K}$, all other cuts are applied. The arrow indicates a chosen cut. b) Kaon identification in $B_s^0 \to \phi\gamma$ events. Optimization ratio ξ versus cut value of $\Delta \log \mathcal{L}_{K\pi}$, all other cuts are applied.

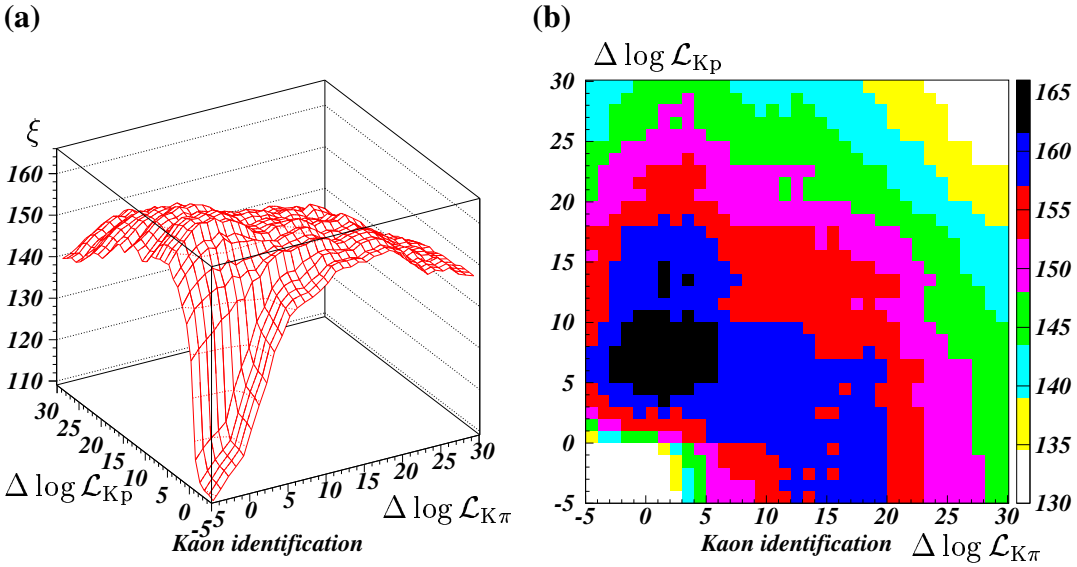

Figure 3: Kaon identification in the case of $B^0 \to K^{*0}\gamma$: a) The dependency of ratio ξ on the cut values of $\Delta \log \mathcal{L}_{K\pi}$ and $\Delta \log \mathcal{L}_{Kp}$. b) Colored projection of a). Cuts are chosen to be $\Delta \log \mathcal{L}_{K\pi} > 0$ and $\Delta \log \mathcal{L}_{Kp} > 5$.

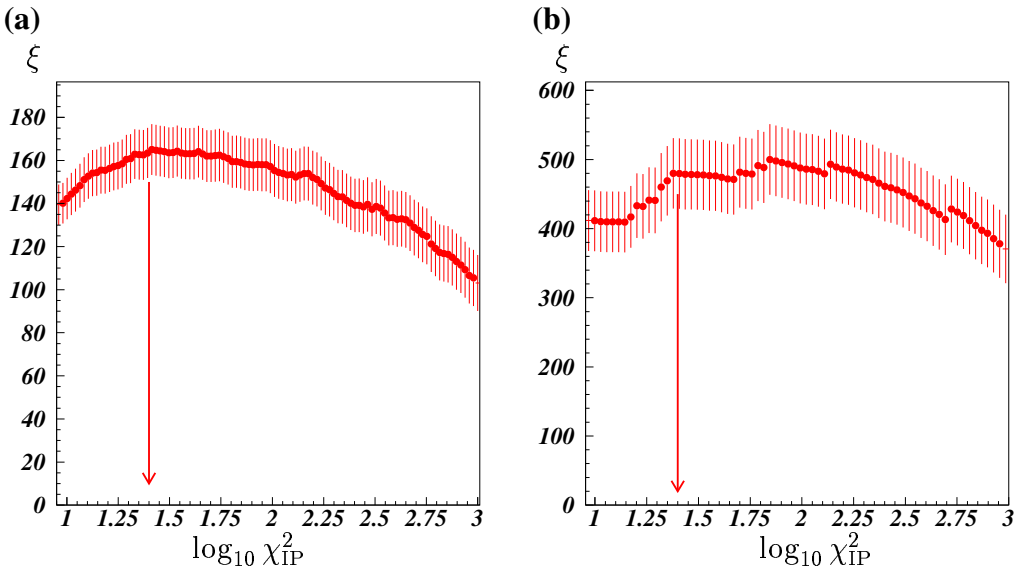

Figure 4: a) The dependency of the ratio ξ on $\chi^2_{\rm IP}$ in case of a) $\rm B^0 \to K^{*0}\gamma$ and b) $\rm B^0_s \to \phi\gamma$ selection. The arrow indicates the chosen cut $\chi^2_{\rm IP} > 25$.

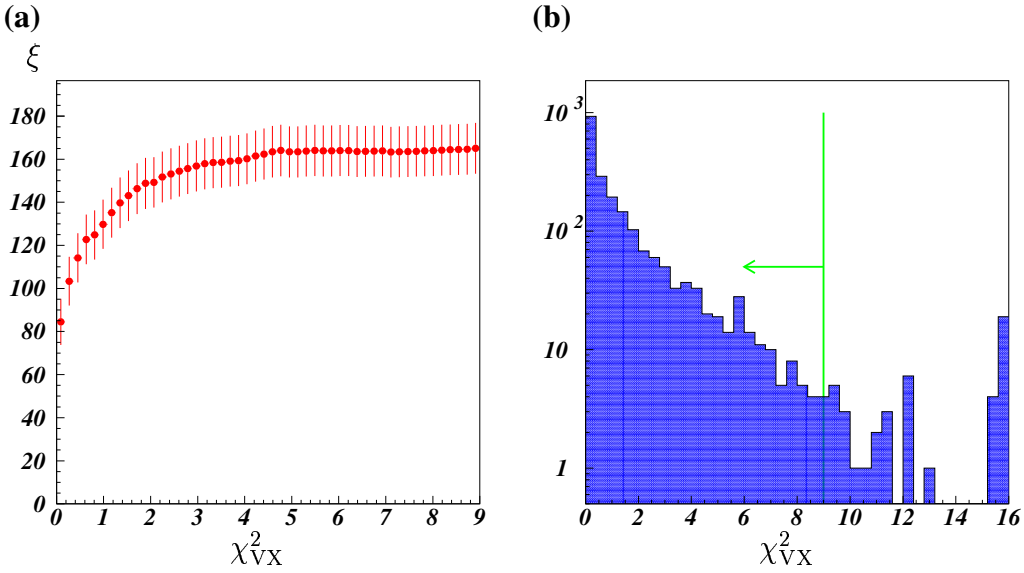

Figure 5: a) The dependency of the ratio ξ on cut value on the $\chi^2_{\rm VX}$ for $\rm B^0 \to K^{*0}\gamma$ selection; b) The distribution of $\chi^2_{\rm VX}$ for $\rm B^0 \to K^{*0}\gamma$ events after all selection cuts.

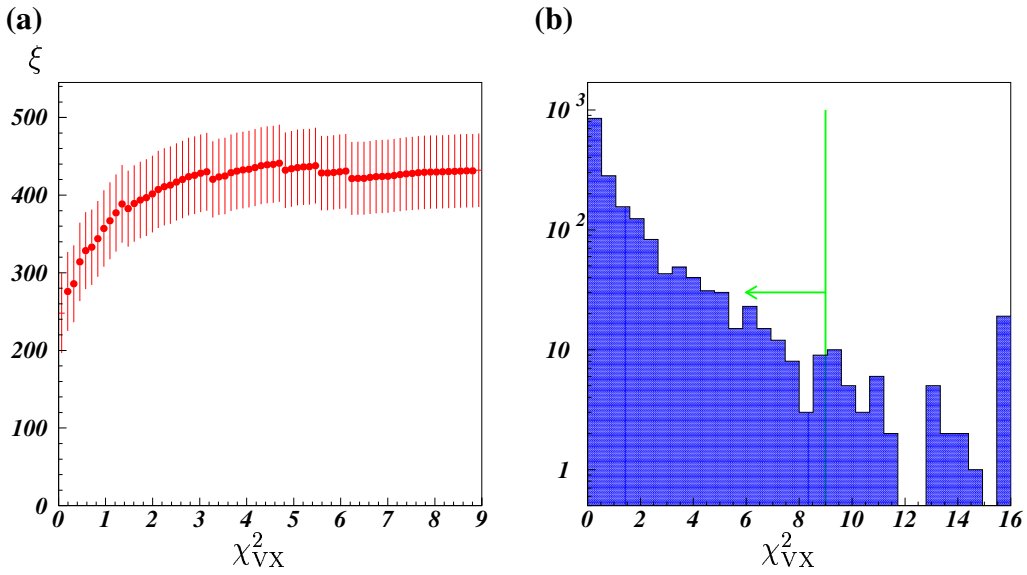

Figure 6: a) The dependency of the ratio ξ on cut value on the $\chi^2_{\rm VX}$ for $\rm B^0_s \to \phi\gamma$ selection; b) The distribution of $\chi^2_{\rm VX}$ for $\rm B^0_s \to \phi\gamma$ events after all selection cuts.

and $\pm 10\ \rm MeV/c^2$ respectively around their nominal masses. The corresponding distributions for the ratio ξ and the invariant mass distributions are shown in Figures 7 and 8.

In order to reconstruct B mesons, the selected $\rm K^{*0}$ and ϕ candidates are combined with a photon candidate. The decay vertex of the $\rm K^{*0}$ (ϕ) is assumed to coincide with the decay vertex of B meson. The production vertex of the B candidate is taken to be the primary vertex with respect to which the B impact parameter, $\rm IP_B$, has the smallest value. The distribution of χ^2-value for this impact parameter, $\chi^2_{\rm IP_B}$, and the corresponding dependency of ξ ratio on the cut value of $\chi^2_{\rm IP_B}$ are shown in Figure 9. The $\chi^2_{\rm IP_B}$ is required to be less than nine.

The angle, $\theta_{\rm B}$, between the momentum of the reconstructed B candidate and its flight path from the production to decay vertices provides a powerful constraint to reject the background. The Figures 10 and 11 represent the dependency of the optimization ratio ξ on the upper cut values of $\theta_{\rm B}$ and its significance[3], $\chi^2_{\theta_{\rm B}}$. The optimal values for the upper cut on $\theta_{\rm B}$ are $8\ \rm mrad$ and and $10\ \rm mrad$ respectively for the $\rm K^{*0}\gamma$ and $\phi\gamma$ final states. The small opening angle between the kaons produced in the $\phi \to \rm K^+K^-$ decay results in a poor ϕ (and therefore $\rm B^0_s$) vertex

[3]The significance $\chi^2_{\theta_{\rm B}}$ has been defined as the χ^2 of the special constrained fit procedure, described in [21–23].

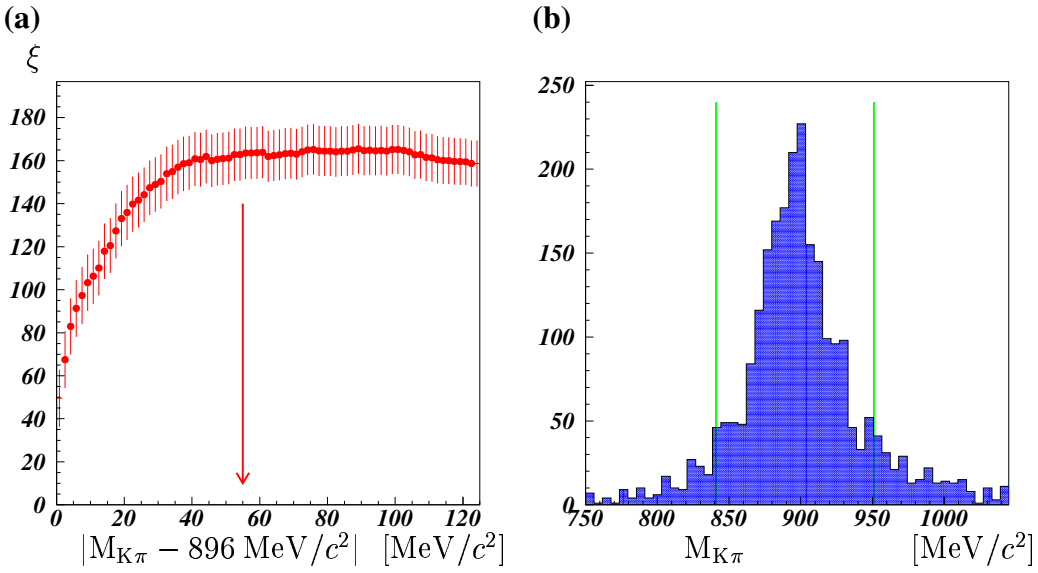

Figure 7: a) The dependency of the ratio ξ on the K^{*0} mass window for $B^0 \to K^{*0}\gamma$ selection. b) The distribution of the K^{*0} invariant mass for $B^0 \to K^{*0}\gamma$ events passing all selection criteria.

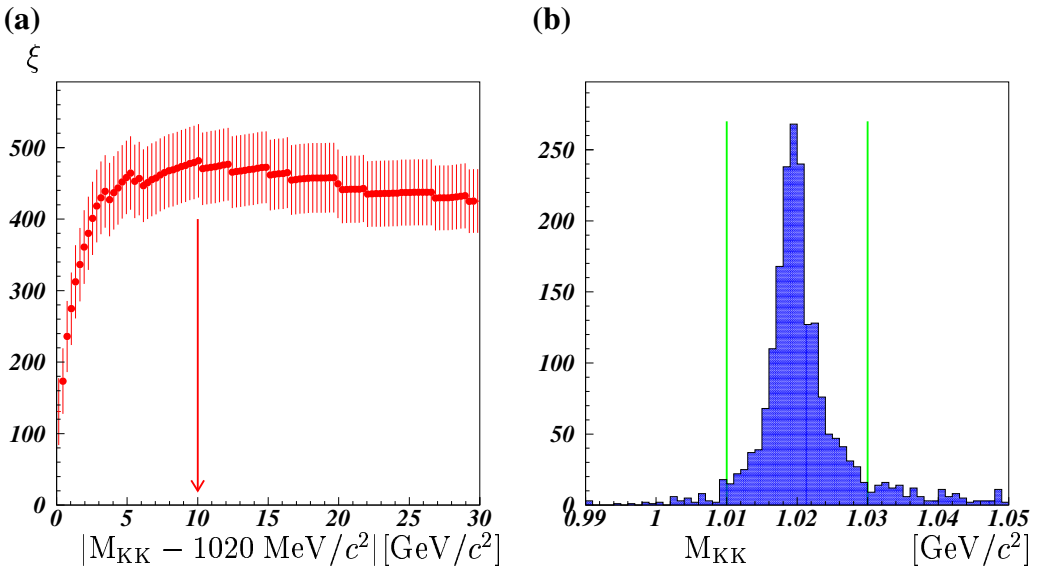

Figure 8: a) The dependency of the ratio ξ on the ϕ mass window for $B_s^0 \to \phi\gamma$ selection. b) The distribution of the ϕ invariant mass for $B_s^0 \to \phi\gamma$ events passing all selection criteria.

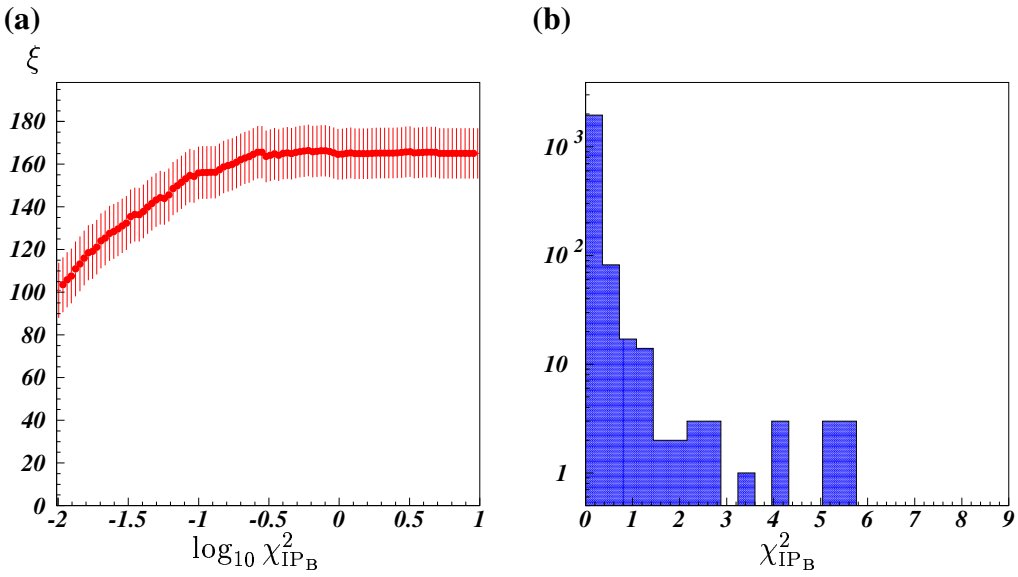

Figure 9: a) The dependency of the ratio ξ on cut value of $\chi^2_{\mathrm{IP_B}}$ for $\mathrm{B}^0 \to \mathrm{K}^{*0}\gamma$ selection. b) The $\chi^2_{\mathrm{IP_B}}$ distribution for $\mathrm{B}^0 \to \mathrm{K}^{*0}\gamma$ events passing all selection criteria.

resolution. This effect is reflected in the looser cut for the of $\mathrm{B}^0_{\mathrm{s}} \to \phi\gamma$ selection. For both final states the optimized value for the upper cut on $\chi^2_{\theta_{\mathrm{B}}}$ is found to be seven $\left(\chi^2_{\theta_{\mathrm{B}}} < 7\right)$.

The background from decays $\mathrm{B}^0 \to \mathrm{K}^{*0}\pi^0$ and $\mathrm{B}^0_{\mathrm{s}} \to \phi\pi^0$ requires special consideration. These decays can mimic the signal if energetic π^0 are identified as a single photon. In order to suppress this background the different polarization of the vector mesons for the signal and background candidates is exploited. The helicity of the K^{*0}/ϕ meson is equal to 0 and ± 1 in $\mathrm{B}_{(\mathrm{d/s})} \to (\mathrm{K}^{*0}/\phi)\,\pi^0$ and $\mathrm{B}_{(\mathrm{d/s})} \to (\mathrm{K}^{*0}/\phi)\,\gamma$ decays. The helicity angle, θ_{H}, is defined as the angle between one daughter of the vector meson (K^{*0}/ϕ) and the reconstructed B meson in the rest frame of the vector meson. The θ_{H} is expected to follow a $\sin^2\theta$ distribution for signals and $\cos^2\theta$ for the correlated background, while it is flat for the combinatorial background. The optimized cut value on $|\cos\theta_{\mathrm{H}}|$ is found to be 0.8 as shown in Figure 12 and Figure 13.

The mass distributions of the selected and triggered [19] B^0 and $\mathrm{B}^0_{\mathrm{s}}$ mesons are shown on Figure 14. The widths of the reconstructed B^0 and $\mathrm{B}^0_{\mathrm{s}}$ are found to be 69.9 ± 2.2 MeV$/c^2$ and 70.9 ± 2.1 MeV$/c^2$. These are dominated mainly by the ECAL energy resolution [17]. The signal mass interval is defined to be

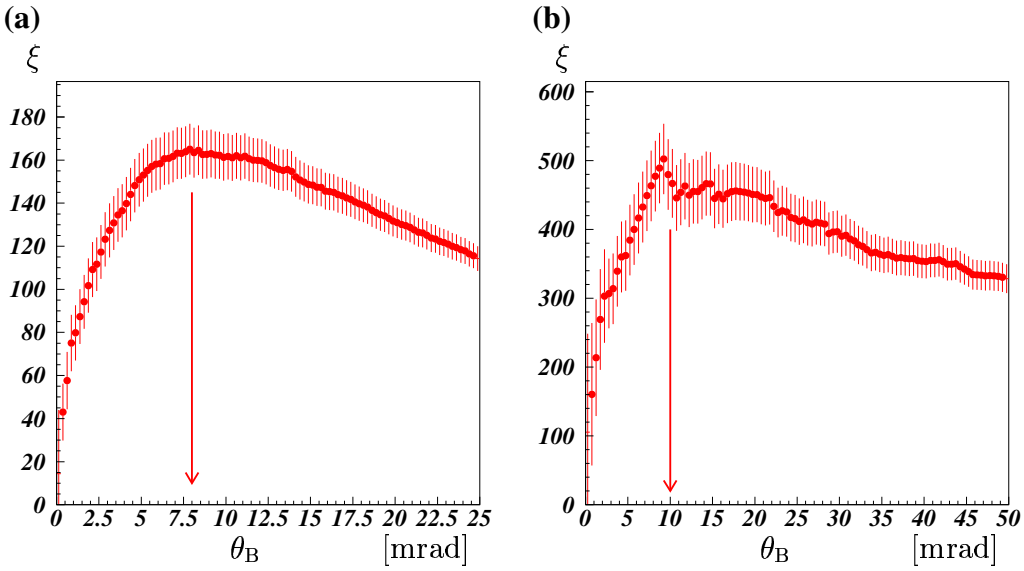

Figure 10: The dependency of the ratio ξ on the cut value of the direction angle θ_B for $B^0 \to K^{*0}\gamma$ (a) and $B_s^0 \to \phi\gamma$ (b) selection respectively.

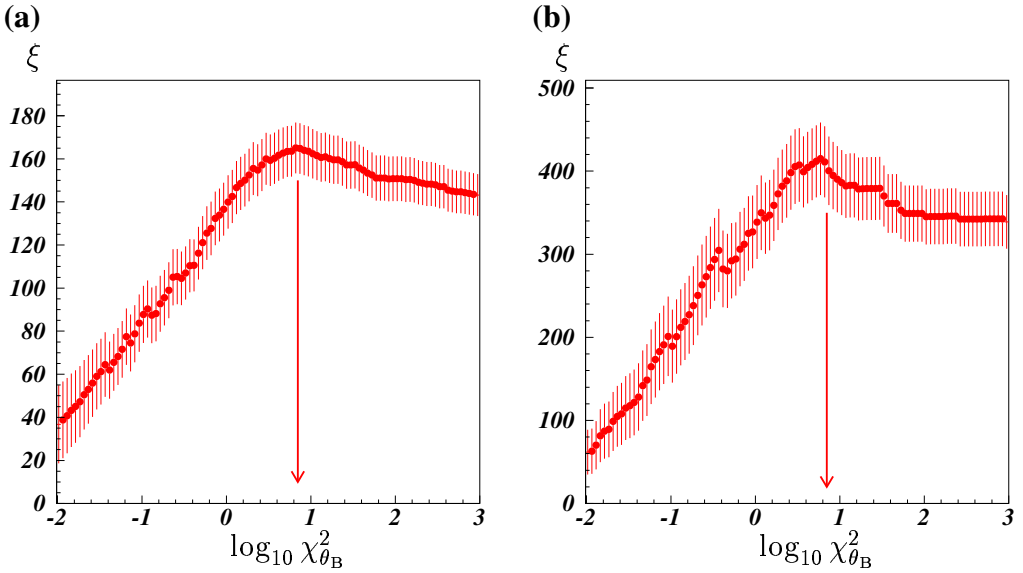

Figure 11: The dependency of the ratio ξ on the cut value of $\chi^2_{\theta_B}$ for $B^0 \to K^{*0}\gamma$ (a) and $B_s^0 \to \phi\gamma$ (b) selection respectively.

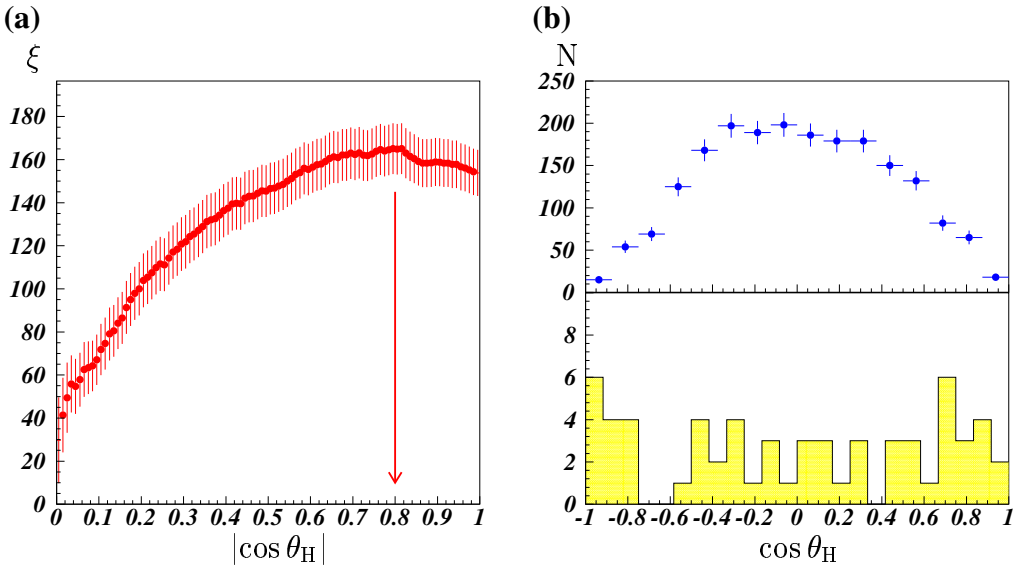

Figure 12: a) The dependency of the ratio ξ on the cut value of $|\cos\theta_{\rm H}|$ for $\rm B^0 \to K^{*0}\gamma$ selection. b) The $\cos\theta_{\rm H}$ distribution for $\rm B^0 \to K^{*0}\gamma$ (top) and for $\rm b\bar{b}$-inclusive (bottom) events passing all selection criteria.

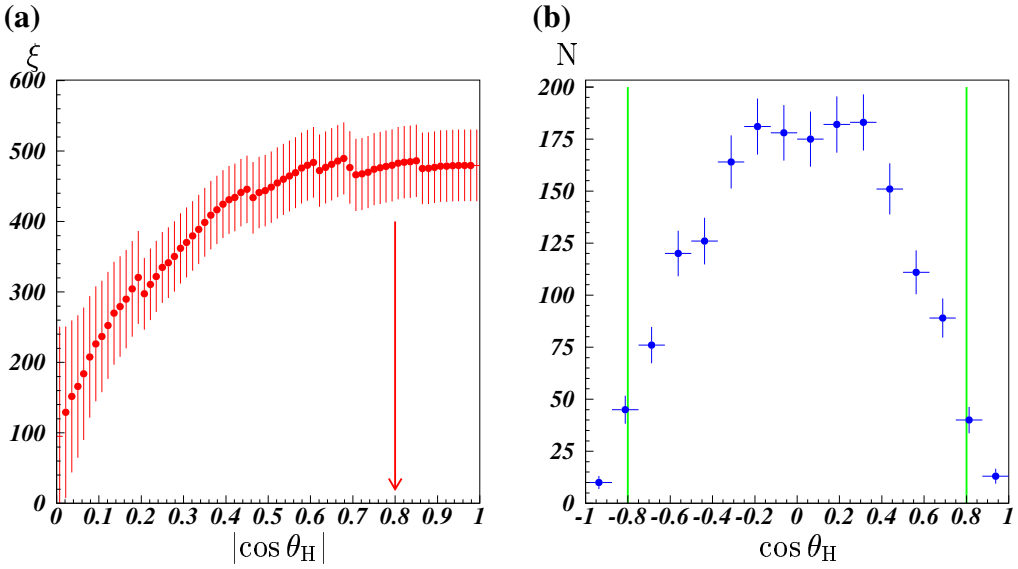

Figure 13: a) The dependency of the ratio ξ on the cut value of $|\cos\theta_{\rm H}|$ for $\rm B_s^0 \to \phi\gamma$ selection. b) The $\cos\theta_{\rm H}$ distribution for $\rm B_s^0 \to \phi\gamma$ events passing all selection criteria.

$\pm 200\ \mathrm{MeV}/c^2$ around the nominal mass of B mesons [24].

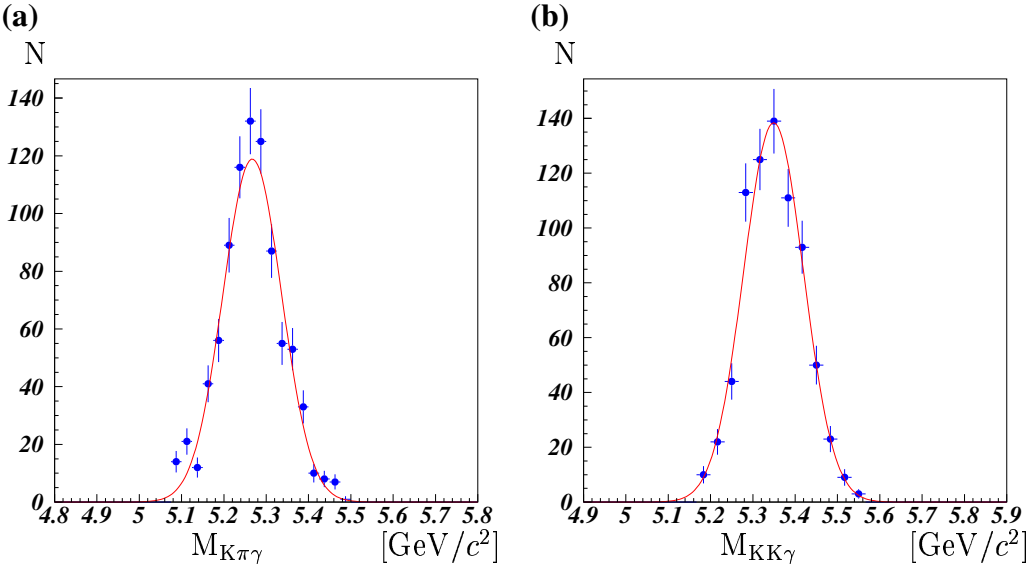

Figure 14: The invariant mass distributions for selected and triggered $\mathrm{B}^0 \to \mathrm{K}^{*0}\gamma$ (a) and $\mathrm{B}^0_\mathrm{s} \to \phi\gamma$ (b) decays respectively.

In the case of the $\mathrm{B}^0 \to \mathrm{K}^{*0}\gamma$ selection, it is possible to see the distinct pattern of the signal and background distributions with the considered sample of 34 million $\mathrm{b\bar{b}}$-inclusive events. The final distribution of these events is shown in Figure 15.

3 Efficiencies and annual yield

The total efficiency is calculated as the fraction of B decays that are triggered, reconstructed and selected with the cuts described above. It can be represented as

$$\varepsilon_{tot} = \varepsilon_{rec} \times \varepsilon_{sel/rec} \times \varepsilon_{trg/sel},$$

where ε_{rec} is the reconstruction efficiency including the geometrical acceptance in 4π solid angle, $\varepsilon_{sel/rec}$ is the efficiency of the offline selection cuts on the reconstructed events and $\varepsilon_{trg/sel}$ is the combined $\mathrm{L0} \times \mathrm{L1}$ trigger efficiency on selected events. The efficiencies obtained are presented in Table 1.

Using the visible branching ratio $\mathrm{BR_{vis}}\left(\mathrm{B}^0 \to \mathrm{K}^{*0}\gamma\right) = 29.0 \times 10^{-6}$ [24] and the probability for a $\mathrm{\bar{b}}$-quark to hadronize into a B^0, $f\left(\mathrm{\bar{b}} \to \mathrm{B}^0\right) = 39\%$, the yield

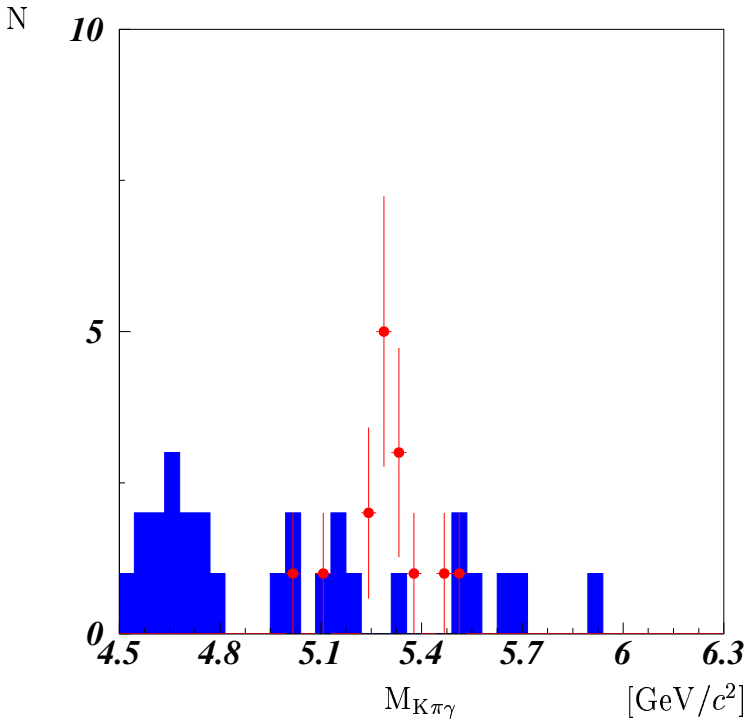

Figure 15: The invariant mass distribution for selected $B^0 \to K^{*0}\gamma$ candidates from the $b\bar{b}$-inclusive sample. The red points indicate true $B^0 \to K^{*0}\gamma$ events and the blue filled histogram represents combinatorial background.

for a nominal annual integrated luminosity of $L_{\rm int} = 2\,{\rm fb}^{-1}$ for $B^0 \to K^{*0}\gamma$ is calculated to be 68k events[4]. Assuming that BR $(B_s^0 \to \phi\gamma)$ = BR $(B^0 \to K^{*0}\gamma)$ and $f\left(\bar{b} \to B_s^0\right) = 10\%$, 11k reconstructed, selected and triggered $B_s^0 \to \phi\gamma$ events are expected.

Provided that the inclusive $b\bar{b}$ background gives the most significant contribution to combinatorial background, the $\mathcal{B}/\mathcal{S}$ ratio can be estimated. The background under the B mass peak is estimated making a linear extrapolation of the number of $b\bar{b}$ inclusive events observed in the wide B mass interval ± 1 GeV$/c^2$ around the nominal B mass. In making this extrapolation a small number of

[4]See [15] and [16] for details.

Table 1: Obtained efficiencies.

Efficiency	$B^0 \to K^{*0}\gamma$	$B_s^0 \to \phi\gamma$
ε_{rec}	5.6%	5.4%
$\varepsilon_{sel/rec}$	11.7%	11.7%
$\varepsilon_{trg/sel}$	45.9%	44.1%
ε_{tot}	0.30%	0.28%

true signal decays had to be removed. The $\mathcal{B}/\mathcal{S}$ ratios are estimated without applying the trigger. In total 41 and 5 background events excluding true signal decays passed the selection criteria for $B^0 \to K^{*0}\gamma$ and $B_s^0 \to \phi\gamma$ decays respectively. Correspondingly, the $\mathcal{B}/\mathcal{S}$ ratio is calculated to be 0.71 ± 0.11 and < 0.95 @ 90% CL. After applying the L0 $\times$ L1 trigger, the $\mathcal{B}/\mathcal{S}$ ratio is estimated to be 0.60 ± 0.16 for $B^0 \to K^{*0}\gamma$ and < 0.55 @ 90% CL for $B_s^0 \to \phi\gamma$.

3.1 Study of the remaining background sources

The nature of background events surviving the selection criteria has been studied in the wide (± 1 GeV/c^2) and narrow (± 200 MeV/c^2) mass intervals for B mesons.

3.1.1 Background for $B^0 \to K^{*0}\gamma$ decays

In order to study background events the mass interval for K^{*0} candidates was enlarged from ± 55 MeV/c^2 to ± 75 MeV/c^2. Background events are classified according to the origin of the charged tracks and photons.

As shown in Table 2, charged tracks can originate either from primary PV (fragmentation processes) or secondary SV (B-decays) vertices. They can also be associated with ghost tracks.

The quality of particle identification is shown in Table 3.

From the data presented in the tables the contribution from ghost tracks can be seen to be 3% only. With the present understanding of track reconstruction within LHCb this type of background is not substantial for these decays. The data in Table 3 suggest particle misidentification is not a significant background either. Only 12% of particles are misidentified. In 78% of events the selected tracks come from the same vertex[5]. So the background consists of mainly $K\pi$-pairs coming

[5]This source of background could be reduced by a tightening of the K^{*0} and ϕ mass windows.

Table 2: Origin of selected charged tracks forming K^{*0} candidates.

		π from		
		Fragmentation	B decays	Ghosts
K from	Fragmentation	2(same PV) 2(different PV)	1	1
	B decays	2	38(same SV) 3(different SV)	0
	Ghosts	1	1	0

Table 3: The quality of particle identification.

		π		
		Misidentified	Identified correctly	Ghosts
Kaons	Misidentified	1	8	0
	Identified correctly	2	37	1
	Ghosts	0	2	0

from the same B decay. It explains the very wide maxima on the dependency of the optimization ratio ξ on the cut values for $\chi^2_{\rm IP}$ and $\chi^2_{\rm VX}$.

Photons are observed to come from merged π^0 in 25 events, real single photons are selected in 24 events and photons are taken from different particles in two events. Partially reconstructed B multiparticle decays are found within 22 of selected events that tend to be in the low mass region and hence do not contribute to the signal mass window. For example $B^{\pm,0} \to K\pi\pi\pi\pi^0$ (or $B^0 \to K\pi\pi^0\pi^0$) decays in the final state where a merged π^0 is identified as a photon and a combination of the charged kaon with one of the pions is found to be consistent with a K^{*0}. Three events are $B^0 \to K^{*0}\pi^0$ with merged π^0 that lie in a signal region.

3.1.2 Background for $B^0_s \to \phi\gamma$ decays.

Five events were selected in the wide mass window. Two of them correspond to $B^0 \to \phi\pi^0$ decays with a merged π^0. One event comes from $B^0 \to \phi {K_S}^0$, where products of ${K_S}^0$ decay are identified as a single photon. Another two events are combinatorial with true ϕ-mesons from B decays. In one case, a merged π^0 is selected from another B decay and in the other case, a photon is reconstructed from many calorimeter deposits from various particles which originate from the

primary vertex.

These 5 events are mainly real ϕ and the major part of the background photons comes from merged π^0.

4 Summary

From this study, the yield for 2 fb^{-1} for $\mathrm{B}^0 \to \mathrm{K}^{*0}\gamma$ decays is expected to be 68k reconstructed events with background to signal ratio 0.71 ± 0.11 (0.60 ± 0.15 after passing L0 $\times$ L1 triggers). For $\mathrm{B}_\mathrm{s}^0 \to \phi\gamma$ decays the annual yield is estimated to be 11.5k with $\mathcal{B}/\mathcal{S} < 0.95$ @ 90% CL (< 0.55 @ 90% CL after L0 $\times$ L1).

The study of the remaining background empasizes the vital importance of the proper identification of photons, in particular the separation of high energy photons from the merged π^0's and the rejection of photon pairs compatible with π^0-decays. Preliminary studies show the capability to reach high background rejection with modest signal losses [25, 26]. These new identification techniques are currently under investigation to be applied for the selection of rare radiative B-decays.

The study of the sensitivity to the CP asymmetry will be presented in a future LHCb note.

5 Acknowledgments

We would like to express our thanks to our colleagues from LHCb Rare decays group for the atmosphere of good will and for kind support of this work. Especially we thank L. Camilleri, V. Egorychev, P. Koppenburg and M. Patel for their constructive comments, M. Knecht and Y. Xie for their useful remarks and O. Deschamps and U. Egede for their invaluable contributions.

Appendix

The optimization ratio ξ defined as

$$\xi = \frac{\mathcal{S}}{\sqrt{\mathcal{S}+\mathcal{B}}}$$

is a multivariable function of the selection cuts values. Here $\mathcal{S}$ is a number of signal events in a signal mass window (in this study it is defined as $\pm 200\ \mathrm{MeV}/c^2$ around known $\mathrm{B}^0_{\mathrm{d/s}}$ mass), $\mathcal{B}$ is a number of background $\mathrm{b\bar{b}}$ inclusive events in the signal mass window. $\mathcal{B}$ is obtained from the all available events in a wide mass region (in the present study $\pm 1\ \mathrm{GeV}/c^2$) excluding true signal events and assuming that background has a flat shape.

The iterative procedure of the cut optimization implies finding the ξ maxima while varying the selection cuts. For the first iteration the cuts described in [15] were applied. The maximum value of ξ is found separately for each cut, keeping the others fixed. The procedure is repeated iteratively until the position of maxima for each particular cut c_i, corresponding to the 2 consequent iterations $(j-1)$ and j, c_i^j and c_i^{j-1}, differ significantly less that the width of the maximum:

$$\left| c_i^j - c_i^{j-1} \right| \ll \left| \frac{1}{\xi} \frac{\partial^2 \xi}{\partial c_i^2} \right|^{-\frac{1}{2}} \tag{2}$$

In case of low statistics special treatment near the optimal point is required. It is possible to release some cuts in order to find the maximum on the other one. For this to be valid the optimized function ξ must change smoothly and be rather broad around the maximum.

Consider two cuts c_1 and c_2 which are to be released. The requirements for allowed changed Δc_1 and Δc_2 are the following:

- Let Δc_1 (with c_2 fixed) give ΔB_1 background events more, and Δc_2 (with c_1 fixed) ΔB_2 events so that $\Delta B_1 \simeq \Delta B_2$. Changes Δc_1 and Δc_2 simultaneously give rise to ΔB events.

- The condition $|\Delta B - \Delta B_1 - \Delta B_2| \ll \min(\Delta B_1, \Delta B_2)$ ensures that cuts c_1 and c_2 belong to a factorization region near the optimum point.

- Additional condition on steps Δc_1 and Δc_2 demands that one doesn't move away from the maximum. It stands $\Delta c_i < \delta c_i$, $i = 1, 2$, where δc_i is the

width of ξ:

$$\delta c_i = \left| \frac{1}{\xi} \frac{\partial^2 \xi}{\partial c_i^2} \right|^{-\frac{1}{2}}$$

Under these conditions it is possible to investigate the function ξ with a number of events sufficient to determine its behaviour near the maximum.

In the case of rather broad maximum of ξ distribution the cut value providing the maximum of the signal efficiency is chosen. Also in this case to simplify the possible cross-checks and studies for common systematics for different channel, the same cut value have been chosen for $\mathrm{B}^0 \to \mathrm{K}^{*0}\gamma$ and $\mathrm{B}_\mathrm{s}^0 \to \phi\gamma$ channels.

References

[1] T. Hurth, T. Mannel, hep-ph/0109041

[2] K. Kiers, A. Soni, G.-H. Wu, *Phys. Rev.* D **62**, 116004 (2000)

[3] D. Atwood, M. Gronau, A. Soni, *Phys. Rev. Lett.* **79**, 185 (1997)

[4] A. Soni, hep-ph/0509180

[5] B. Aubert *et al.*, *Phys. Rev.* D **72**, 051103 (2005)

[6] K. Abe *et al.*, hep-ex/0507059

[7] D. Atwood, T. Gershon, M. Hazumi, A. Soni, *Phys. Rev.* D **71**, 076003 (2005)

[8] S.W. Bosch, G. Buchalla, hep-ph/0408231

[9] D. Mohapatra *et al.*, *Phys. Rev. Lett.* **96**, 221601 (2006)

[10] B. Aubert *et al.*, hep-ex/0607099

[11] M. Nakao *et al.*, *Phys. Rev.* D **69**, 112001 (2004)

[12] B. Aubert *et al.*, *Phys. Rev.* D **70**, 112006 (2004)

[13] T.E. Coan *et al.*, *Phys. Rev. Lett.* **84**, 5283 (2000)

[14] A. Ali and A. Parkhomenko, hep-ph/0105302

[15] G. Pakhlova and I. Belyaev, CERN-LHCb-2003-090

[16] R. Antunes Nobrega *et al.*, CERN-LHCC-2003-030

[17] S. Amato *et al.*,CERN-LHCC-2000-036

[18] O. Deschamps *et al.*, LHCb-2003-091

[19] R. Antunes Nobrega *et al.*, CERN-LHCC-2003-031

[20] S. Amato *et al.*, CERN-LHCC-2000-037

[21] G. Raven, LHCb-2003-118

[22] E. Aslanides *et al.*, LHCb-2004-001

[23] B. Viaud, CPPM-T-2003-06

[24] K. Hagiwara *et al.*, *Phys. Rev.* D **66**, 010001 (2002)

[25] S. Barsuk, private communication

[26] B. Delcourt, private communication